IMPROVEMENTS IN AEROSOL RETRIEVAL FOR ATMOSPHERIC CORRECTION

S.M. Adler-Golden, M.W. Matthew, A. Berk, M.J. Fox, J. Lee and A.J. Ratkowski[*]

Spectral Sciences, Inc., Burlington, MA
[*]Air Force Research Laboratory, Hanscom AFB, MA

ABSTRACT

First-principles atmospheric correction that converts Visible-NIR-SWIR spectral imagery to surface reflectance requires an estimate of the scene visibility / aerosol optical depth. This paper describes aerosol upgrades to FLAASH, a first-principles atmospheric correction algorithm developed by Spectral Sciences, Inc. and the US Air Force Research Laboratory. FLAASH utilizes an automated band ratio method for retrieving an average scene visibility from dark pixels. The visibility estimate is combined with a MODTRAN™ aerosol representation to describe the atmosphere. Recent FLAASH upgrades improve both visibility retrieval and atmospheric correction accuracy. These result in better handling of highly off-nadir viewing geometries, high aerosol optical depths and sensors lacking infrared spectral channels.

Index Terms— hyperspectral, multispectral, correction, compensation

1. INTRODUCTION

Accurate first-principles atmospheric correction (or compensation) that converts Visible-NIR-SWIR hyperspectral or multispectral imagery (HSI or MSI) data to surface reflectance units requires an estimate of the scene visibility / aerosol optical depth. This paper describes some recent aerosol upgrades to the FLAASH code, a first-principles atmospheric correction algorithm developed by Spectral Sciences, Inc. in collaboration with the US Air Force Research Laboratory and other US Government agencies [1,2]. FLAASH uses MODTRAN™ [3] radiation transport modeling for deriving both surface spectral reflectance and atmospheric properties. A commercial version of FLAASH is available within the ENVI software package from ITT Visual Information Solutions.

FLAASH utilizes an automated band ratio method for retrieving an average scene visibility from dark pixels. The visibility estimate is then combined with one of the standard MODTRAN™ aerosol types to describe the atmosphere. Recently, a research version of FLAASH was upgraded to improve both visibility retrieval and atmospheric correction accuracy, and to enable visibility retrieval in problematic cases where the current FLAASH retrieval method fails. These improvements result in better handling of highly off-nadir viewing geometries, scenes with high aerosol optical depth, sensors lacking infrared spectral channels and scenes lacking both dark vegetation and water bodies.

The original FLAASH method starts with an assumed visibility and identifies dark pixels using an infrared wavelength (typically near 2.1 μm) at which reflectance retrieval is ordinarily insensitive to visibility. Visibility is then retrieved by requiring that a bandpass reflectance ratio for these pixels matches a predetermined empirical value. However, the pixel selection method is inappropriate when there is high aerosol loading or an unusually long path to the sensor, or when the method is applied to shorter wavelengths. In the upgraded algorithm, the pixel selection is dependent on the trial visibility, enabling identification of useful dark vegetation and water bodies in these cases.

An important feature of FLAASH for high-aerosol scenes and off-nadir viewing is its modeling of the adjacency effect that mixes the spectrum of the direct line-of-sight pixel with its neighbors in the diffuse transmittance term of the radiation transport equation. For better treatment of this effect, a more accurate adjacency point spread function (PSF) has been implemented within the single-scattering approximation, accounting for wavelength dependence as well as for asymmetry in off-nadir viewing geometries.

The upgrades in the new version of FLAASH, called "FLAASH-2007", are illustrated with applications to MSI and HSI data sets. Of particular interest is imagery acquired by NASA's EO-1 Hyperion sensor under extreme off-nadir conditions, including data collected near Davis, CA in June 2005 [4]. These images were taken at an off-nadir viewing angle of nominally 63°, corresponding to only a 9° angle above the horizontal at the ground and a viewing line-of-sight through approximately six air masses.

2. ALGORITHM DETAILS

2.1. Adjacency Correction

FLAASH solves for the pixel surface reflectance ρ using the at-sensor radiance equation [2,5]

$$L^* = a\rho/(1-\rho_e S) + b\rho_e/(1-\rho_e S) + L^*_a \qquad (2.1)$$

Here ρ_e is a spatially averaged surface reflectance, S is the spherical albedo of the atmosphere from the ground, L^*_a is the radiance backscattered by the atmosphere, and a and b are coefficients that solely depend on atmospheric and geometric conditions. The second term corresponds to the radiance from the surface that is diffusely transmitted into the sensor, giving rise to the "adjacency effect". The averaging implied in ρ_e is a convolution with a spatial point spread function (PSF). Strictly speaking, different PSFs apply when ρ_e appears in the numerator and denominator; however, since $\rho_e S$ is generally very small, we approximate the denominator PSF with the numerator PSF, which describes the upward diffuse transmittance. ρ_e is estimated from an approximate form of Eq. (2.1),

$$L_e{}^* = (a+b)\rho_e/(1-\rho_e S) + L^*{}_a \qquad\qquad (2.2)$$

Here $L_e{}^*$ is the radiance image convolved with the PSF. Eq. 2.1 is then solved for ρ.

We use the term "kernel" for FLAASH's simplified mathematical representation of the upward diffuse transmittance PSF. The transmittance is governed by the path atmospheric extinction, the scattering albedo for each scattering event and the value of the scattering phase function. For a stratified atmosphere, the phase function depends on the relative contributions of scatterers as a function of altitude. For a cloud-free atmosphere, the relative strengths of aerosol and Rayleigh scattering dictate the shape of the PSF. The kernel calculation in FLAASH-2007 accounts for both of these sources and models the radial asymmetry that occurs in off-nadir viewing geometries.

The sensor-to-ground vertical extinction optical depth consists of four components, the aerosol absorption (t_{aa}) and scatter (t_{as}), the Rayleigh scatter (t_{ms}), and atmospheric molecular absorption (t_{ma}):

$$t = t_{aa} + t_{as} + t_{ms} + t_{ma} \qquad\qquad (2.3)$$

The adjacency PSF is angular- and wavelength-dependent on the two scattering terms, t_{as} and t_{ms}. Expressions for Rayleigh and aerosol scattering optical depth are well known [6]. The phase function for aerosol scattering is approximated by a two-term Henyey-Greenstein analytical function. We assume an inverse exponential altitude dependence of scatterers for both aerosol and Rayleigh terms. Then, the *single-scatter* aerosol and Rayleigh adjacency kernels, $<t_{as}>$ and $<t_{ms}>$ respectively, are defined as products of the line-of-sight scattering optical depth and a density-weighted average phase function. The total adjacency kernel is then expressed by the normalized sum of $<t_{as}>$ and $<t_{ms}>$.

The shape of the total kernel for a 63° off-nadir angle at the ground with an assumed visibility of 100 km is shown in Figure 1. For this visibility, the fractional contribution from Rayleigh scattering is less than that from aerosol for all wavelengths above ~0.5 μm. Therefore the 355 nm kernel is primarily from Rayleigh scattering, while the 2577 nm kernel is dominated by the aerosol scattering. Higher aerosol loadings (lower visibility) cause the kernel to be even more heavily dominated by the aerosol component. Note that at both wavelengths the kernel is asymmetric on this 20m x 20m square pixel grid.
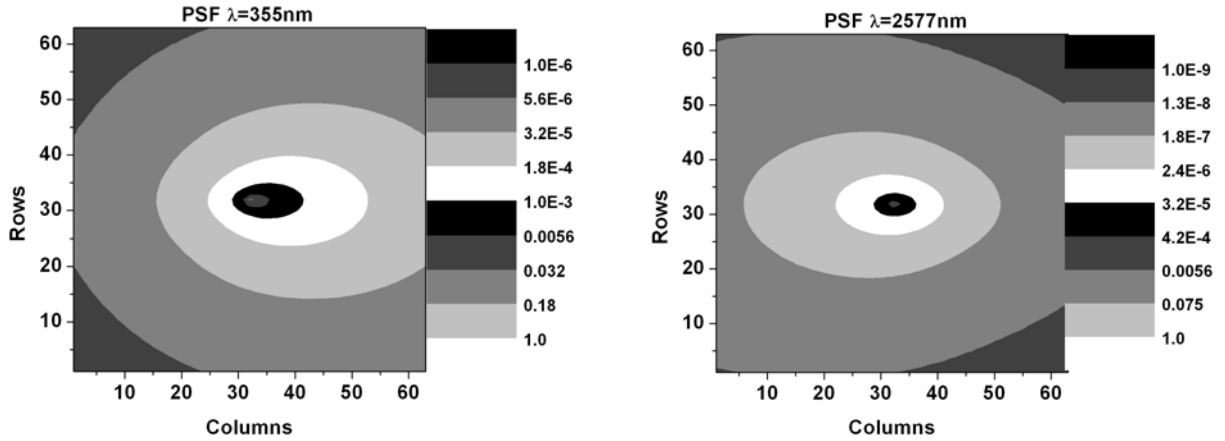

Figure 1. Adjacency kernels at 355 nm (left) and 2577 nm (right). The sensor is located to the left of the center in these simulations. Image pixels are 20m x 20m. The aerosol optical depth is 0.067 and the visibility is 100 km. The Rayleigh contribution to the kernel is 84% at left and 5% at right.

2.2. Visibility Retrieval

2.2.1. Retrieval Bands and Reflectance Ratios

The automated visibility retrieval algorithm in FLAASH is based on the assumption that for a particular type of dark terrain, a certain pair of bandpasses has a characteristic, known reflectance ratio. Different bandpasses and ratios define land and water pixel methods, as described by Rochford *et al.* [7]. The land pixel method is based on the work of Kaufman *et al.* [8,9], and assumes that dark green vegetation has a characteristic reflectance ratio in Landsat bands 3 and 7 (red and ~2.1 μm, respectively). The default band 3 to band 7 reflectance ratio assumed by FLAASH is 0.45, which is an average for vegetation in both moist and dry climates. The commonly quoted ratio of 0.5 yields slightly higher visibilities. The vegetation pixels are chosen as those having a band 7 reflectance value less than a cutoff of ~ 0.1 and also satisfying a red-to-VNIR ratio criterion that discriminates against shadow and water.

The FLAASH water pixel method uses the Landsat infrared bands 4 and 7 with a nominal reflectance ratio of 1.0 and a band 4 reflectance cutoff of 0.03. It presumes that the source of water reflectance in the infrared is spectrally flat glint or foam. However, a better estimate of the glint spectrum, at least, may be derived from the Fresnel equations using the wavelength-dependent index of refraction for water. The calculated reflectance ratio for a water surface at 2.1 μm *vs.* 0.8 μm (n=1.289 *vs.* n=1.326) is 0.81 for incident angles between 0 and 30 deg. This ratio also appears to be a better estimate for foam than the spectrally flat assumption [10].

Other spectral band pairs have been proposed for visibility retrieval. The Landsat (1,7) (blue, 2.1 μm) band pair was suggested as an alternative for use with green vegetation by Kaufman *et al.* [8,9]; the reflectance ratio is ~ 0.25. Combining this ratio with the Landsat band 3 to band 7 ratio suggests that the (1,3) (blue, red) band pair (reflectance ratio ~ 0.5) may be used with data that are limited to visible wavelengths.

2.2.2. Dark Pixel Selection and Scene Visibility Computation

The automated method of selecting dark pixels for aerosol retrieval in FLAASH is via a bandpass cutoff that defines the maximum allowable reflectance. In the two-band vegetation method, the selection is made at ~ 2.1 μm. At this wavelength, the reflectance tends to be insensitive to the assumed visibility, so a reasonable visibility estimate suffices for the pixel selection. Trial atmospheric corrections are conducted for these selected pixels, and an error figure of merit (FOM) is computed. We use a FOM that should have a zero crossing at the true visibility, namely, the average difference between the computed and empirical reflectance ratios. In this case, the scene visibility may be derived by linearly interpolating the FOM to zero.

With the water pixel and blue-red retrieval methods, the retrieval pixels are selected using a reflectance cutoff at a shorter wavelength, where there is greater sensitivity to the assumed visibility. In addition, for long-slant-path viewing even the 2.1 μm band is sensitive to visibility. Here the proper way to perform the pixel selection is to atmospherically correct the entire scene at the cutoff-bandpass for each trial visibility, and then to apply the cutoff to create unique sets of selected pixels for each trial visibility. This new method is implemented in FLAASH-2007.

3. RESULTS AND DISCUSSION

For validation of the new algorithms in FLAASH-2007 and comparisons with the older ENVI FLAASH version, visibility retrievals were performed for a diverse set of hyperspectral and multispectral images, and with various reflectance ratio and cutoff parameter settings. We used the same ENVI interface for both versions of FLAASH. Since this interface provides more convenient control over parameters and bandpasses with multispectral data than with hyperspectral data, the hyperspectral images were degraded to multispectral (Landsat-7) bands for the purpose of visibility retrieval. All of the views are nadir views except for the Sacramento Valley, CA image measured by the EO-1 Hyperion sensor, as described elsewhere [4]. Aerosol scale heights were taken as 1.0 km for the two littoral scenes and 1.5 km for the interior land images.

A summary of visibility results from different FLAASH versions and retrieval methods is given in Table 1. FLAASH-2007 tends to yield slightly lower values than ENVI FLAASH for a given reflectance ratio and cutoff. It appears that the main difference is in the adjacency kernel. The new, more accurate kernel, has a narrower central peak, reducing the magnitude of the adjacency scattering effect and, therefore, requiring a lower visibility for equivalent total path scattering when the dark pixel areas are small. With FLAASH-2007, there is better overall consistency between the vegetation and water-based visibility retrievals using the Table 1 vegetation reflectance ratio of 0.50 rather than 0.45; the former yields slightly higher visibilities. Dependence of the vegetation method on the cutoff value is generally slight, except with the Landsat Davis image, where a cutoff of 0.08 gives the closest results to a ground truth visibility measurement of ~ 70 km [7].

Additional ground truth visibility measurements are available for the Coleambally (New South Wales, Australia) data cube, for which the reported visibility is slightly over 100 km, and for the Hyperion off-nadir image of Sacramento Valley, where the visibility, measured at Davis, was in the neighborhood of 185 km. In both cases, the vegetation method with the 0.50 ratio gave good results. In comparing ground truth and retrieved visibilities, it is important to note that the sensitivity of reflectance spectra to the visibility value at very high visibilities (clear weather) is modest since the aerosol optical depth scales with the *reciprocal* of the visibility.

A comparison of the vegetation- and water-based retrievals, from the last two columns of Table 1, is shown in the Figure 3 plot of the visibility reciprocal. The Landsat Davis image is omitted due to the very small number of identified water pixels, and the Hyperion Sacramento Valley image is omitted for reasons discussed below. For the remainder, the correlation between visibilities derived from vegetation and water is very strong.

Table 1. Visibility Retrievals (km) from FLAASH. Veg = Kaufman *et al*. vegetation method (Landsat bands 3 and 7); Water = water method (bands 7 and 4); Blue-red = visible vegetation method (bands 1 and 3); f = retrieval failure. Reflectance cutoff is applied to the second band in the pair. Values in parentheses are questionable due to calibration uncertainty or surface specularity (see text).

Method, ratio, cutoff			Veg 0.45, 0.10	Water 1.0, 0.03	Blue-red 0.50, 0.04	Veg 0.50, 0.08	Water 0.8, 0.03
FLAASH Version			ENVI 4.3	ENVI 4.3	2007	2007	2007
Image	Description	Truth	Retrieved	Retrieved	Retrieved	Retrieved	Retrieved
Hyperion Coleambally	Agricultural	>100	66	f	300	71	f
AVIRIS Monterey	Littoral		34	54	22	42	54
Landsat Fresno, CA	Agricultural		29	54	34	32	41
Landsat San Francisco	Mixed		36	65	37	38	48
AVIRIS Tampa Bay	Littoral		24	41	(13.4)	24	37
AVIRIS Virgin Mts.	Desert, water		f	66	f	f	44
AVIRIS Ft. AP Hill	Fall foliage		41	61	71	49	56
Landsat Davis, CA	Mixed	70	78	43	36	73	34
AVIRIS SCAR	Rural smoky		6.6	f	(12.9)	6.4	5.7
Hyperion Sacr. Valley	Agric. long slant	>130	f	f	f	123	(36)

The 0.8 value for the water reflectance ratio is preferable to the 1.0 value according to the Fresnel equation derivation, and appears to yield somewhat more realistic-looking water pixel spectra; however, it slightly increases the small but consistent disparity between the land- and water-based visibility retrievals (the latter are higher by an average of around 20%). The cause of this disparity is not clear. One possibility is that the typical aerosols may have somewhat different optical properties than the MODTRAN™ aerosol models used by FLAASH; this could introduce a bandpass-dependent error. The maritime model was assumed for the two littoral scenes, of Tampa Bay and Monterey Bay, while the rural model was assumed for the rest. Use of the maritime model for the Tampa Bay scene is supported by previous work [11]. Another possibility is that the average reflectance ratio for vegetation in these scenes is slightly larger than 0.50.

The blue-red method produced generally reasonable results with most of the vegetation-containing images. The notable exceptions, the Tampa Bay and SCAR images, are both from AVIRIS data that are more than ten years old, predating instrument upgrades that appear to have improved its calibration as well as the sensitivity. The 1993 Tampa Bay data have a positive radiance offset in the blue region [11], while the 1995 SCAR data show a negative short-wavelength spike when plotted in reflectance units [1].

The FLAASH-2007 upgrades enabled reasonable retrieval of visibility from land pixels in the highly off-nadir Hyperion Sacramento Valley image. Retrieval of visibility from water-covered fields was much less successful because the effective reflectance spectrum of water bodies becomes brighter and skewed to the blue at high off-nadir angles. This effect is associated with reflected skyshine, caused by the dramatic increase in specular reflectance of a water surface from ~2% at nadir to 40% at 81.3° off-nadir. As a result, the water pixel method produces unrealistically low visibility. In addition, visibility was successfully retrieved from water pixels in the smoky SCAR image that ENVI FLAASH was unable to identify.

The reflectance ratio and cutoff values listed in Table 1 for FLAASH-2007 provide the best overall consistency between the vegetation- and water-derived visibilities, and will be used as the new defaults. The results suggest that in nadir views the typical accuracy of aerosol optical depth retrieval in FLAASH-2007 should be ~ 0.01 km^{-1} in units of inverse visibility.
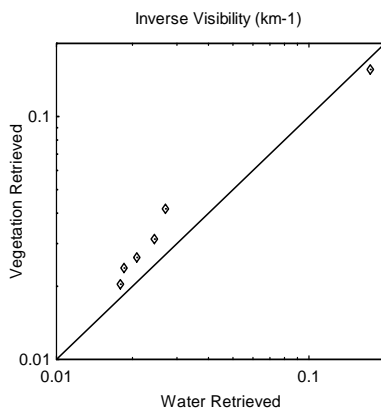
Figure 3. FLAASH-2007 land- and water-based visibility retrieval comparison, from the Table 1 values. The straight line corresponds to exact agreement between the retrievals.

5. REFERENCES

[1] Matthew, M.W., S.M. Adler-Golden, A. Berk, G. Felde, G.P. Anderson, D. Gorodetzky, S. Paswaters and M. Shippert, "Atmospheric Correction of Spectral Imagery: Evaluation of the FLAASH Algorithm with AVIRIS Data," SPIE Proceeding, Algorithms and Technologies for Multispectral, Hyperspectral, and Ultraspectral Imagery IX (2003).

[2] Adler-Golden, S., A. Berk, L. S. Bernstein, S. Richtsmeier, P. K. Acharya, M. W. Matthew, G. P. Anderson, C. L. Allred, L. S. Jeong and J. H. Chetwynd, "FLAASH, a MODTRAN4 Atmospheric Correction Package for Hyperspectral Data Retrievals and Simulations," presented at the Seventh Annual JPL Airborne Earth Science Workshop, Pasadena, CA (January 12, 1998).

[3] Berk, A., G.P. Anderson, L.S. Bernstein, P.K. Acharya, H. Dothe, M.W. Matthew, S.M. Adler-Golden, J.H. Chetwynd, S.C. Richtsmeier, B. Pukall, C.L. Allred, L.S. Jeong and M.L. Hoke, "MODTRAN4 Radiative Transfer Modeling for Atmospheric Correction," SPIE V. 3756, Denver CO (1999).

[4] Adler-Golden, S. M., L. S. Bernstein, M. W. Matthew, R. L. Sundberg and A. J. Ratkowski, "Atmospheric Compensation of Extreme Off-Nadir Hyperspectral Imagery from Hyperion," Proc. SPIE Vol. 6565, Algorithms and Technologies for Multispectral, Hyperspectral, and Ultraspectral Imagery XIII, Sylvia S. Shen, Paul E. Lewis, Eds., pp. 65651P (2007).

[5] Vermote, E., D. Tanre, J.L. Deuze, M. Herman and J.J. Morcrette, "Second Simulation of the Satellite Signal in the Solar Spectrum (6S)," 6S User Guide Version 6.0, NASA-GSFC, Greenbelt, Maryland (1994).

[6] Atzberger, C., "Remote Sensing through the atmosphere – Physical principles and effects," Atmospheric Effects on Satellite Images, Verlag für Wissenschaft und Forschung, Berlin, Germany, ISBN 3-89700-013-X, 267 (2002).

[7] Rochford, P.A., P.K. Acharya, S.M. Adler-Golden, A. Berk, L.S. Bernstein, M.W. Matthew, S.C. Richtsmeier, S. Gulick and J. Slusser, "Validation and Refinement of Hyperspectral/Multispectral Atmospheric Correction Using Shadowband Radiometers," IEEE Trans. Geosci. Remote Sens., 43, 2898-2907 (2005).

[8] Kaufman, Y.J., A.E. Wald, L.A. Remer, B.-C. Gao, R.-R. Li and L. Flynn, "The MODIS 2.1-μm Channel-Correlation with Visible Reflectance for Use in Remote Sensing of Aerosol," IEEE Trans. Geosci. Remote Sens., 35, 1286-1298 (1997a).

[9] Kaufman, Y.J., D. Tanré, L.A. Remer, E.F. Vermote, A. Chu and B.N. Holben, "Operational remote sensing of tropospheric aerosol over land from EOS moderate resolution imaging spectroradiometer," J. Geophys. Res., 102, pp. 17051-17067 (1997b).

[10] Moore, K.D., K.J. Voss and H.R. Gordon, "Spectral reflectance of whitecaps: Their contribution to water leaving radiance," J. Geophys. Res., 105, pp. 6493-6499 (2000).

[11] Adler-Golden, S.M., P.K. Acharya, A. Berk, M.W. Matthew and D. Gorodetzky, "Remote Bathymetry of the Littoral Zone From AVIRIS, LASH, and QuickBird Imagery," IEEE Trans. Geosci. Remote Sens., 435, 337-347 (2005).